Mon. Not. R. Astron. Soc. **000**, 000–000 (0000) Printed 5 February 2008 (MN LATEX style file v1.4)

Faint galaxies close to QSOs with damped Lyman-α absorption systems

Alfonso Aragón-Salamanca,[1] Richard S. Ellis,[1] and Kieran S. O'Brien[2]
[1] *Institute of Astronomy, Madingley Road, Cambridge CB3 0HA, England*
[2] *Royal Greenwich Observatory, Madingley Road, Cambridge CB3 0EZ, England*

Accepted —. Received —; in original form —

ABSTRACT

We have obtained very deep near-infrared images in the fields of 10 QSOs whose spectra contain damped Lyman-α absorption (DLA) systems with $1.7 < z_{\rm abs} < 2.5$. The main aim of our investigation is to provide new constraints on the properties of distant galaxies responsible for the DLA absorption. After subtracting the point spread function associated with the QSO light, we have detected galaxies very close to the QSO line of sight (projected distance 1.2–1.3 arcsec) in two fields. These sources therefore represent promising candidate galaxies responsible for the DLA absorption. Placed at the absorber's redshift, the impact parameter is $10h_{50}^{-1}$ kpc and the luminosity is close to L_K^*. Such parameters are consistent with the hypothesis, verified for metallic systems at lower redshift, that slowly-evolving massive galaxies produce at least some of the absorption systems of high column density in QSO spectra out to beyond $z \simeq 2$. In addition to detecting these candidate DLA galaxies, the radio-loud QSOs in our sample show a significant excess of sources on larger scales ($\theta \simeq 7$ arcsec); this excess is not present in the radio-quiet QSO sightlines. We calculate that such an excess could be produced by luminous galaxies in the cores of clusters associated with radio-loud QSOs. Both results confirm that deep imaging of selected QSOs can be a powerful method of finding samples of likely $z \simeq 2$ galaxies. Follow-up near-infrared spectroscopy is required to secure galaxy redshifts and star formation rates, while deep HST imaging can determine sizes and morphologies, providing valuable information on galaxy properties at large look-back times.

Key words: cosmology: observations — galaxies: evolution — infrared: galaxies — quasars: absorption lines

1 INTRODUCTION

Considerable progress has been made in recent years in understanding the evolutionary behaviour of starlight from distant field galaxies. Systematic redshift surveys (Ellis et al. 1995, Lilly et al. 1995) have provided large datasets from which the evolution of the luminosity function of galaxies has been directly determined to redshifts $z \simeq 1$. Such studies are complemented by smaller, but independent surveys based on the absorbing properties galaxies present to background luminous QSOs (Bahcall & Peebles 1969). Following the pioneering work of Bergeron and Boissè (1990), Steidel & Dickinson (1995) have identified those galaxies responsible for the MgII absorption seen in the sightlines to 68 QSOs and have thus derived luminosity functions and rest-frame colours for the absorbing field galaxies at a mean redshift of $z \simeq 0.7$.

It is gratifying that both techniques, viz surveys that select galaxies by their *emission* and those via their *absorption*, give consistent results for the evolutionary behaviour of massive galaxies to $z \simeq 1$ (Steidel & Dickinson 1995, Ellis 1995). Surprisingly little evolution is seen in both the colours and luminosities of such galaxies indicating they were already in place at large look-back times. The principal difference between the techniques lies in understanding the origin and fate of the numerous star-forming dwarfs seen in the redshift surveys (Ellis 1995); such galaxies do not appear to be prominent in the metallic absorber-selected samples.

The slow evolution of massive galaxies to $z \simeq 1$ has important implications for the likely detection of similar systems at higher redshift, particularly for early-type disk galaxies whose star formation rates are expected to increase slightly with redshift. Limited field spectroscopy has been performed beyond $z = 1$ (Cowie, Hu & Songaila 1995) but QSO absorption samples are available in abundance. Indeed, some constraints on the nature of galaxies responsible for

high z metallic systems are available from statistical studies of a few MgII systems (Steidel et al. 1995, private communication) and a sample of more distant CIV absorbers (Aragón-Salamanca et al. 1994). Although no spectroscopic identifications have yet been made for these systems, the implied luminosities and impact parameters are consistent with continuation of the trends found at lower redshift.

Of particular interest in this regard is the nature of the material which produces the damped Lyman alpha absorption (DLA, Wolfe et al. 1986). Conventional wisdom holds that such systems arise infrequently when the disk of an absorbing galaxy presents a small impact parameter to the QSO. Statistical analyses indicate the abundance of MgII, CIV and DLA systems is consistent with a single population of massive galaxies whose volume density approximates that seen today, the principal difference arising in the cross-section. If this is the case, deep imaging in good seeing will be required to isolate the galaxies responsible for the DLA systems. Although this explanation is not accepted universally (see, e.g., Yanny & York 1992), any constraints on the properties of galaxies close to the QSO sightline where a DLA absorber may be present will be of interest.

This paper begins to explore the possibilities observationally. In Section 2 we present new infrared imaging observations of 10 QSO sightlines each chosen to contain a damped Lyman alpha absorption. Section 3 analyses the distribution of faint sources found as a function of projected distance from the QSO, and discusses two promising cases where the DLA absorber may have been found. The implications are briefly discussed and Section 4 presents our conclusions.

2 THE DATA

The QSOs for this study have been selected from a compilation of confirmed damped Lyman-α systems kindly provided by Max Pettini (Table 1). We selected all the DLA systems with $1.5 < z_{\rm abs} < 2.5$ and $z_{\rm abs} \ll z_{\rm em}$ in the $8^{\rm h} < {\rm R.A.} < 15^{\rm h}$ right ascension range. We imaged 10 QSOs out of the 11 in the Pettini et al. list that fulfill these criteria, the exception being Q1409+095 which was not observed due to the limitations in available telescope time. Out of the 10 observed QSOs, 6 are optically selected with no reported radio emission; the remaining 4 are radio loud (Hewitt & Burbidge 1993). We shall refer to these as the 'radio quiet' and 'radio loud' samples respectively.

The QSOs were imaged in the K-band using the 256×256 InSb infrared camera IRCAM3 on the 3.8 m UK Infrared Telescope on Mauna Kea during the nights of February 24th–27th 1995. All nights were clear and photometric, with good seeing conditions ($0.5''$–$1.2''$). The pixel scale was $0.3''\,{\rm pixel}^{-1}$. Details of the infrared exposures are given in Table 1. Exposure times were chosen to ensure the detection of galaxies as faint as $0.3L^*_K$ at $z_{\rm abs}$ assuming no evolution. We adopt $H_0 = 50\,{\rm km\,s^{-1}Mpc^{-1}}$ and $q_0 = 0.5$ throughout, and $M^*_K = -25.1$ form Mobasher, Sharples and Ellis 1993. The K-corrections used in this paper followed procedures described more fully in Aragón-Salamanca et al. (1994).

The observing procedure involved numerous dis-registered short exposures in a 3×3 pattern of step size $\simeq 7''$. The exact telescope offsets included a random component of $\simeq$ 1–$2''$ amplitude in the right ascension and declination directions which avoids producing images at exactly the same position with consequent problems in flat-fielding (see ahead). The individual image exposures were 60 s, composed of six 10 s background-limited sub-exposures. Dark frames were obtained at frequent intervals with the same exposure times and subtracted from the science images.

The median* of individual images taken over a $\simeq$ 10 minute period around a given observation produces a very good flat-field that yields a uniformity of better than 3–5 parts in 10^5 on the final images.

To improve the sampling of the point spread function (PSF), we utilised the fact that the fields were imaged in many dis-registered positions with fractional pixel shifts thus using information on smaller spatial scales. We artificially divided each pixel in four to produce a scale of $0.15''\,{\rm pixel}^{-1}$. The resampled images were registered (using sub-pixel shifts) and median combined. The final images have well-sampled PSFs with seeings listed in Table 1, and cover $1' \times 1'$ at their maximum depth. The images were reduced using our own software based on the FIGARO package written by Keith Shortridge.

Photometric calibrations were secured by repeated observations of standard stars in the UKIRT faint JHK standards list (Casali & Hawarden 1992), yielding absolute photometry whose internal accuracy is better than 0.01 mag *r.m.s.*

In order to detect objects as close as possible to the QSO sightlines, we subtracted a suitably scaled PSF from the QSO images using the DAOPHOT package in IRAF. To determine the PSF we used bright stars in the same image when available. Given the relatively small field of view, this was not always possible. In those cases where no bright star was present in the field, we determined the PSF from a bright star in an image with better seeing and convolved it with a two dimensional Gaussian of the appropriate σ, ellipticity and orientation so that the resulting PSF would have the right shape parameters (as determined from the QSO image itself). The success of this procedure depends critically on the QSO brightness, but we achieved residuals fainter than the limiting magnitude of the images (see ahead) at radii larger than 0.6–$2''$ from the QSO centre. Table 1 lists the minimum radius $\theta_{\rm min}$ for which reliable source detection was possible. The region $\theta < \theta_{\rm min}$ was patched out and excluded from further analysis. Our procedure is arranged so as to subtract the maximum amount of QSO light by matching the PSF parameters to those of the QSO image. This is helpful in revealing discrete sources "under" the PSF rather than residual QSO "fuzz".

Figure 1 shows the images before and after PSF subtraction. In the case of Q1100−264, —the brightest QSO in the sample— the PSF subtracted image shows some diffuse residual light which results from limiting the diameter of the subtracted PSF to 35 pixels (5.25 arcsec). Note that

* Strictly speaking, instead of the median, we used the Biweight central location estimator, which behaves like the median when the number of data points is large, but produces a better S/N for relatively small samples. See Beers et al. (1990) for a detailed description of this statistical estimator.

Table 1. The QSO sample.

QSO	$z_{\rm em}$	$z_{\rm abs}$ DLA	$z_{\rm abs}$ Metals	Exp. time (seconds)	Seeing FWHM ($''$)	$K_{\rm lim}$ (mag)	$\theta_{\rm min}$ ($''$)
0836+113	2.696	2.465	0.787[a]	12960	0.9	21.7	0.6
0841+129 [r]	> 2.51[b]	1.861, 2.375, 2.477		12480	1.0	21.7	0.9
1100−264 [r]	2.145	1.839	0.359, 1.219	6480	1.0	21.3	2.0
1136+122	2.894	1.789	0.317, 2.074	6480	0.9	21.3	1.0
1151+068	2.762	1.774	0.684, 1.819, 2.024	6480	1.1	21.3	1.6
1215+333 [r]	2.606	1.999		11820	1.2	21.7	1.2
1223+178	2.936	2.466		12960	0.9	21.7	1.4
1244+347	2.500	1.860		6780	0.9	21.3	1.5
1331+170 [r]	2.081	1.773	0.745, 1.328, 1.446	8400	0.9	21.4	2.0
1406+123	2.970	2.248		11280	1.0	21.7	1.4

[r] Radio-loud.
[a] Only confirmed metallic absorption systems at $z_{\rm abs}^{\rm metals} \neq z_{\rm abs}^{\rm DLA}$ are listed. For multiple systems, the mean redshift is given (from Junkkarinen, Hewitt & Burbidge 1991; and Hewitt & Burbidge 1993).
[b] 0841+129 is a BL Lac object. Its emission redshift is a lower limit determined from the highest redshift absorption system detected in its spectrum.

the bright star in the Q0836+113 shows the same diffuse structure.

In order to construct the K-selected galaxy samples, automated object detection was performed using the APM software (Irwin 1985) in the STARLINK PISA implementation. An object was detected in the final K images when 6 or more connected pixels had counts larger than 3σ above the background. Adjacent objects were de-blended following the algorithm described by Irwin (1985). The software outputs positions, integrated fluxes, orientation and shape parameters for the detected objects. Integrated photometry in a $2.5''$ diameter aperture was obtained using the PHOTOM package in STARLINK. This procedure is preferable to using the APM magnitudes directly because it provides a local estimation of the sky. We choose a small aperture for the photometry since, given the good seeing conditions, this gives an adequate approximation of the total magnitude while substantially reducing uncertainties from sky subtraction.

Photometric random errors were determined following the procedure described in Aragón-Salamanca et al. (1994). Briefly, we first divided the total integrations in several sub-exposures, and examined the scatter in the photometry for individual objects. Second, we used the sky variance near each object, since for the high K-band background this should be the dominant source of error. Both methods agreed closely, yielding typical random errors $\simeq 0.10$–0.12 at $K \simeq 20$ and $\simeq 0.20$–0.25 at $K \simeq 21$. For each field we adopted that limiting magnitude (Table 1) whose photometric errors are less than 0.3 mag inside the $2.5''$ apertures. The cumulative number counts to these limiting magnitudes show no sign of incompleteness, and are compatible with the published K-band number counts (Gardner, Cowie & Wainscoat 1993). The chosen limiting magnitudes are quite conservative and ensure that no spurious sources that might have been introduced in the catalogues by the automatic detection algorithm were kept.

3 ANALYSIS

3.1 Radial distribution of sources

Following a similar analysis to that of Aragón-Salamanca et al. (1994), we next studied the distribution of sources as a function of angular separation θ from the QSO. Figure 2(a) shows the radial distribution of sources for the combined sample of all 10 QSOs, both in numbers to our adopted K limits and the factor by which the source density exceeds the Gardner, Cowie and Wainscoat (1993) field number counts. There is good agreement between the measured number of sources and that expected from the field number counts at radii larger than $\simeq 10''$. At smaller radii there is, however, a marginal excess. Interestingly, when the QSO sample is split according to radio quiet (6 QSOs) and radio loud (3 QSOs and one BL Lac object), significant differences are seen. Whereas the radial distribution of associated sources for the radio quiet sample is compatible with a uniform distribution (Figure 2(b)), that for the radio loud QSO fields shows an excess of sources at radii $\theta \lesssim 7$ arcsec (Figure 2(c)). In order to quantify the statistical significance of these results, we carried out Kolmogorov-Smirnov tests on the distribution comparing these with a uniform distribution. For the combined QSO sample, the deviation from a uniform distribution is significant only at the 85% level. The sources in the radio-quiet QSO sample show deviations significant at 39%, while the sources in the radio-loud QSO fields are significant at the 99.5% level. These results are consistent with the error bars in Figure 2. While the latter significance is still not formally very high given the sample size, the difference between the two sub-samples suggests that the excess of sources is unlikely to arise from galaxies associated with the DLAs whose properties across the entire sample show no such distinction.

The radial extent of the excess ($\simeq 7$ arcsec, corresponding to $\simeq 60$ kpc at $\langle z_{\rm abs} \rangle = 2.06$) implying cross-sections larger than expected if DLA absorption is produced by the inner, denser galaxy regions (Steidel et al. 1994). Such radial distances are also much larger than those at which neutral hydrogen column densities exceed 10^{21} cm in present day

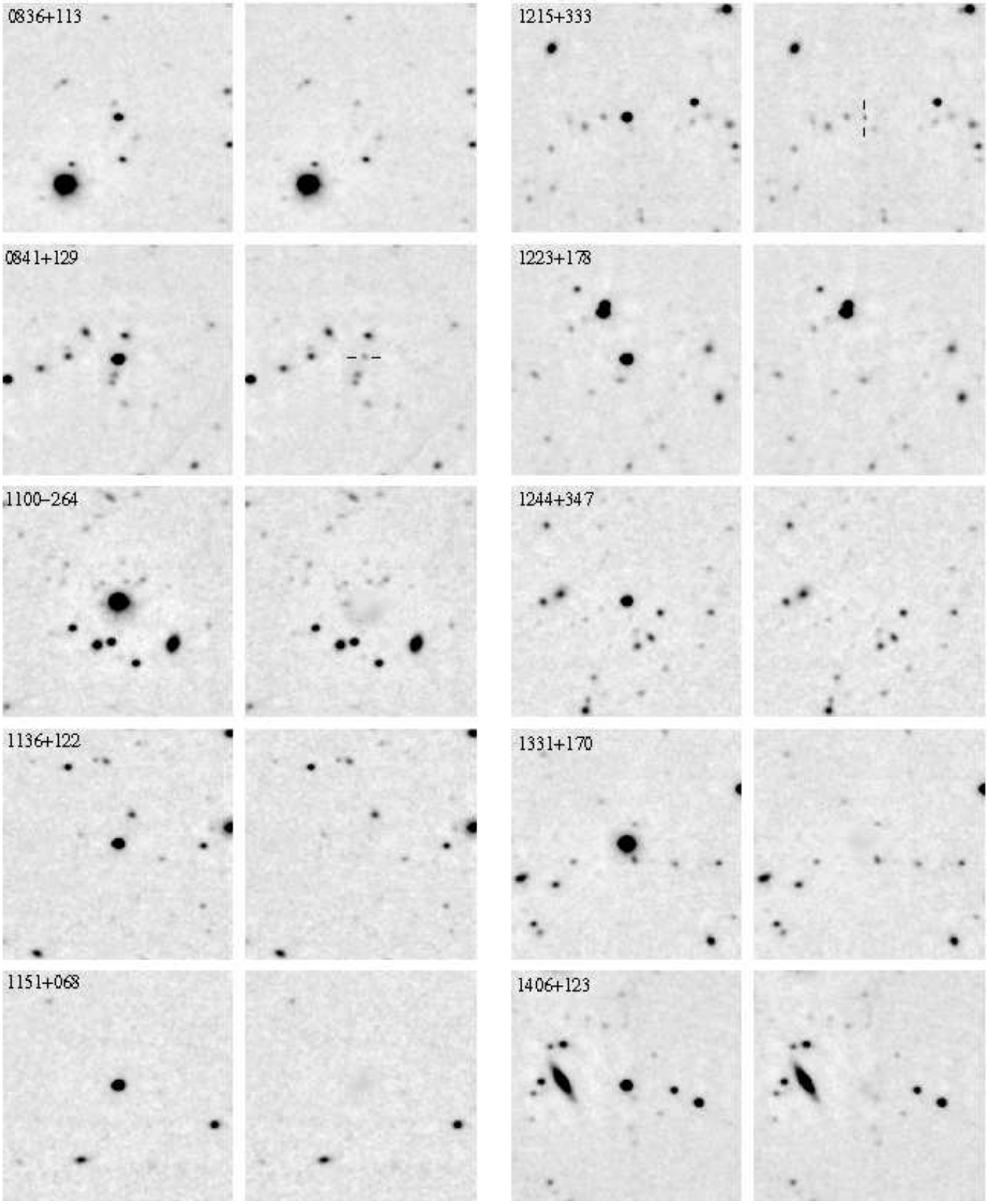

Figure 1. Deep infrared K-band images of the QSOs listed in Table 1 before (left) and after (right) PSF subtraction. North is up, East is left. Each frame is $1' \times 1'$. The two DLA galaxy candidates discussed in Section 3.2 have been marked.

galaxies (Rao & Briggs 1993). Of course this does not preclude the possibility that the excess might be associated with galaxies *clustered* with the ones producing the Lyman alpha absorption, but the difference in behaviour of the radio loud and radio quiet QSO sightlines argues against this.

An important consideration at this point is the fact that some of the QSO spectra show absorption line systems (in particular MgII and CIV) at redshifts lower than those of the DLA (Table 1). As MgII absorption lines at $z \lesssim 1$ are produced by relatively luminous galaxies with characteristic distances from the QSO line of sight $\simeq 70\,$kpc (Bergeron & Boissé 1991; Steidel, Dickinson & Persson 1994, Steidel & Dickinson 1995), some of the excess could be associated with such galaxies. However, in our sample the number of lower redshift absorption systems in radio loud QSOs does not differ significantly from that of radio quiet QSOs, so the presence of an excess in the former and not in the latter is unexplained. Moreover, given the lower redshift of the other metallic absorption systems, we would expect them to be, on average, at somewhat larger radii form the QSO. Indeed, for the one case in our QSO sample where the galaxy producing a low redshift MgII absorption has been identified (Q1100−264, $z_{\rm abs}^{\rm MgII} = 0.359$), the absorbing galaxy is 12 arcsec SE from the QSO (Bergeron & Boissé 1991), thus outside the $\theta \lesssim 7\,$arcsec region where the excess has been detected. Taken collectively, these arguments suggest that if the excess measured close to the radio loud QSO sightlines is real, it is probably largely associated with the QSOs, i.e. at $z_{\rm em}$. This result is consistent with the observation that radio loud QSOs at $z \simeq 0.5$ are frequently situated in cluster environments (cf. Yee & Green 1987; Ellingson, Yee & Green 1991).

The physical scale over which the excess is seen might be understood if we are seeing luminous galaxies in the cores of distant groups or proto-clusters centred around the QSO. Since we would only be able to detect the most luminous, concentrated components of such distant systems, the excess seen would be both of limited significance at our K limit and be compactly distributed. To illustrate this effect at the mean redshift of the radio loud objects ($\langle z_{\rm em}\rangle = 2.37$), we have taken deep K-band images of rich clusters of galaxies at $z = 0.31$ from the study of Barger et al. (1995) and used these to simulate the appearance of a non-evolving cluster observed under the same conditions, and reaching the same depths as our QSO images. We find that we would detect only 2–3 of the brightest cluster galaxies inside a circle of 7 arcsec radius, with an average luminosity of $\langle M_K\rangle \simeq -25.7$, i.e., about 0.5 magnitudes brighter than L_K^*. Figure 3 shows the absolute magnitude distribution of all the galaxies found with a distance $1 < \theta < 7\,$arcsec from the radio loud QSOs, assuming they are at $z_{\rm em}$. In total there are 16 objects, and we would expect $\simeq 5$ from the field K counts indicating an excess of $\simeq 11$ objects or 2.8 objects per radio loud QSO, with an average absolute magnitude $\langle M_K\rangle \simeq -25.9$. The absolute magnitude distribution of the excess objects observed ($M_K \lesssim -26.5$) is $\sim 1\,$mag brighter than would be expected on the basis of present-day brightest cluster galaxies, suggesting some luminosity evolution from $z \sim 2.4$ to $z \sim 0$. Such evolution would not be unreasonable over a $\simeq 10\,$Gyr period, depending on the star formation history of the galaxies. Note, however, that without accurate correction for field contamination there is some uncertainty

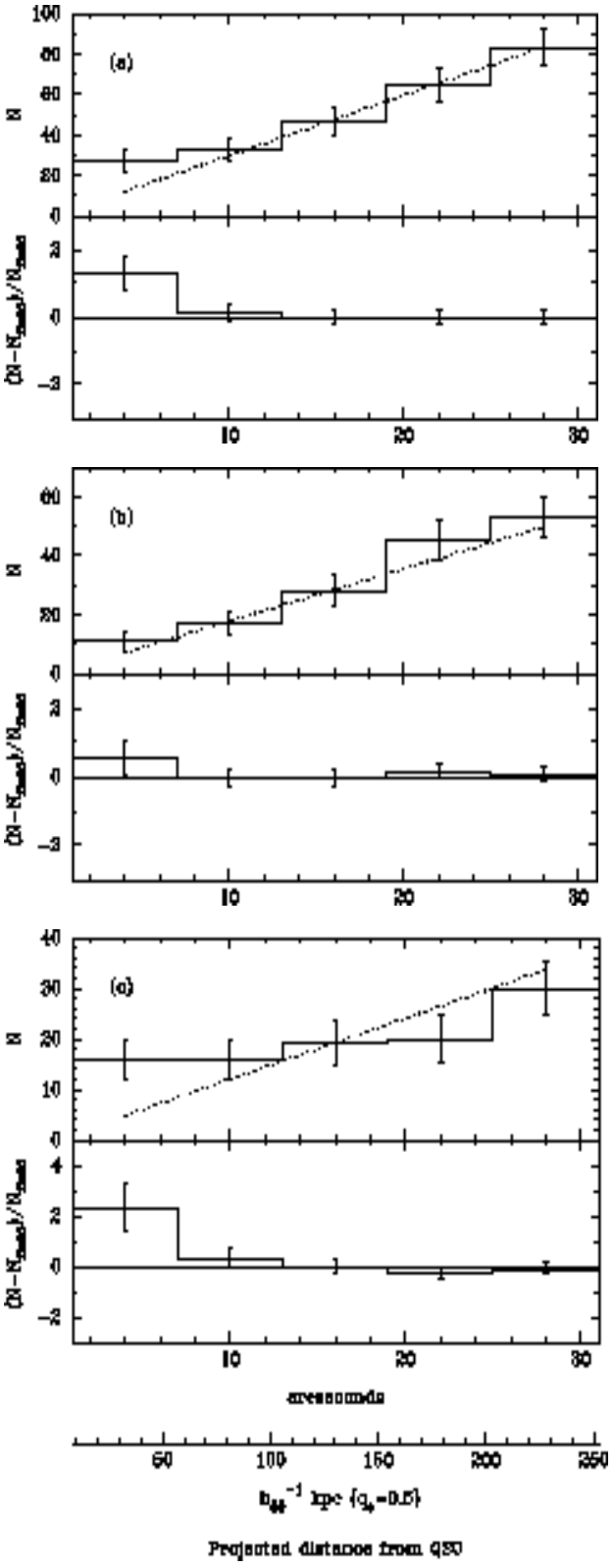

Figure 2. **(a)** The summed distribution of faint sources close to the QSOs as a function of projected radial distance in direct numbers (top) and in terms of the multiplicative excess over the field counts (bottom). The dotted line in the upper panel shows the expected field galaxy counts (see text). **(b)** As (a) but for the radio-quiet QSOs. **(c)** As (a) but for the radio-loud QSOs.

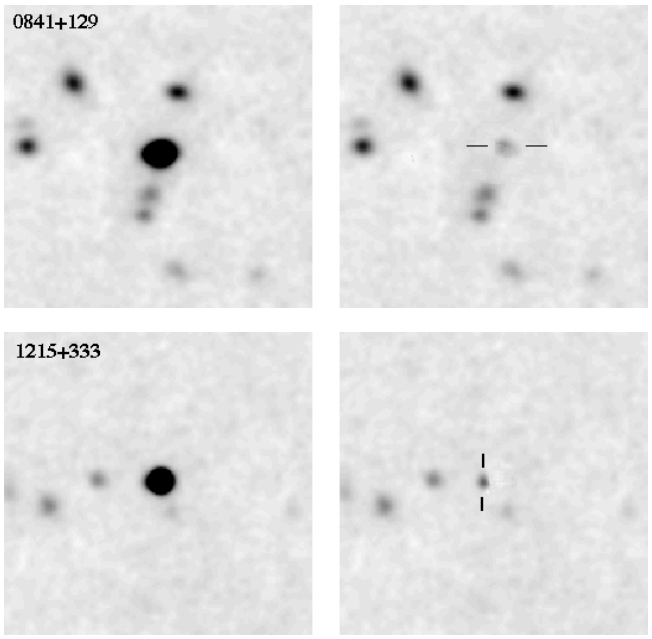

Figure 4. Enlargement of the K-band images presented in Figure 1 for 0841+129 and 1215+333 showing the DLA candidate absorber galaxies. Each frame is $30'' \times 30''$.

Figure 3. Absolute magnitude distribution of all the galaxies found with a distance $1 < r < 7$ arcsec from the radio loud QSOs, assuming they are at $z_{\rm em}$.

in the intrinsic magnitude distribution of the excess objects. Given the size of the sample, it is beyond the scope of this paper to attempt building an "uncontaminated" luminosity function using the field galaxy number counts.

3.2 Objects under the QSO PSF: New DLA galaxy candidates

The primary aim of our observations was to search for candidate galaxies close to the QSO sightline that might be responsible for DLA absorption. Our PSF subtraction procedure reveals galaxies very close to the sightlines of Q0841+129 and Q1215+333, two of the radio-loud objects. Notwithstanding the excess population discussed earlier, these are promising candidate absorbers (Figure 4).

A $K = 19.9$ galaxy was found $1.2''$ NW of the BL-Lac object 0841+129 ($z_{\rm em} > 2.51$), which has three DLA systems at $z_{\rm abs} = 1.8610$, 2.375 and 2.477 (Hazard, private communication). At the average redshift of the DLAs $\langle z_{\rm abs} \rangle = 2.237$, the observed angular distance corresponds to an impact parameter $\simeq 10$ kpc. At that redshift, the galaxy would be about 0.5 mag brighter than a present-day L^*_K galaxy.

A $K = 20.1$ galaxy appears $1.3''$ E of Q1215+333 ($z_{\rm em} = 2.606$), which has a DLA system at $z_{\rm abs} = 1.999$[†]. If the galaxy is at the absorption redshift, its impact parameter would be $\simeq 11$ kpc, and its luminosity would be close to present-day L^*_K.

There are no other known metallic absorption line systems at redshifts lower than that of the DLA systems in either of these two lines of sight. Specifically, intermediate resolution spectroscopy is available in the range $\lambda\lambda$3330–4810 (2.5Å resolution) and $\lambda\lambda$3100–11000 (4–7Å resolution) for Q0841+129 (Hazard, private communication). For Q1215+333, Wolfe et al. (1993) published good quality 1Å resolution spectroscopy in the range $\lambda\lambda$3500–4850 and 2.5Å resolution spectroscopy in the $\lambda\lambda$6625–7325 range which reveal no lower redshift metallic absorption systems.

Given the average K-band field number counts, the limiting magnitudes of the images, and $\theta_{\rm min}$ for the PSF subtraction, the probability of finding two galaxies as close as the ones found here is $\lesssim 2\%$ for the complete QSO sample making the two galaxies promising candidates for the DLA absorption. Assuming this is the case, their luminosities are comparable to those of the lower redshift galaxies responsible for the metal line absorbers, but with smaller impact parameters. This is certainly consistent with the hypothesis that different classes of absorbers trace the same population of galaxies with different cross sections. The DLA systems would then be associated with the inner, denser regions, while metallic lines and Lyman limit systems sample the more tenuous and extended haloes (Steidel et al. 1994).

Of course, this conclusion is not yet convincing given the majority of the DLA systems in our sample have no obvious visible counterpart. At lower redshift, Steidel et al. (1994) have imaged two DLA absorbers at $z_{\rm abs} = 0.3950$ and 0.6922 and found one to be a low surface brightness galaxiy (which would certainly not be detected at our redshifts) whereas the other has $L > 0.25\,L^*$. This disparity in galaxy properties, together with the difficulty of identifying sources closer to the distant QSO sight lines than $\theta_{\rm min}$ may explain the low success rate in finding luminous counterparts.

When the excess of sources found in the radio-loud QSO sightlines is taken into account, the probability of finding very close companions to the QSOs ($\simeq 8\%$ for the whole survey) increases slightly. In other words, the two DLA can-

[†] This absorber was the subject of an infrared spectroscopic study by Elston et al. (1991), who claimed a detection of [OII]λ3727 and Hβ emission at the absorber's redshift. This detection was not confirmed by subsequent studies, and it is now believed to have been spurious (Lowenthal 1995, private communication).

didates might be a subset drawn from the clustered component around the radio-loud QSOs. Obtaining redshifts is the only means of solving these ambiguities. Given the faintness of the objects and their suspected redshift range, the best hope resides in near-infrared spectroscopy, particularly if they are star-forming galaxies whereupon the most likely emission lines would be redshifted into the JHK windows. The very high sky background in the near infrared has been a major obstacle in such work thus far, but the forthcoming availability of purpose-built infrared spectrographs, including those offering OH-suppression, may render such observations feasible in the near future.

4 SUMMARY

We have obtained very deep ($K_{\rm lim} \simeq 21.3$–21.7) images in good seeing conditions of the fields of 10 QSOs with damped Lyman-α absorption systems in the $1.7 < z_{\rm abs} < 2.5$ range. The main aim is to constrain the properties of those galaxies responsible for the DLA absorption and, more generally, to find samples of high redshift galaxies for evolutionary studies. From the analysis of those images, several results emerge:

1. For two of the QSOs, point spread function subtraction techniques reveal the existence of one galaxy in each case very close to the QSO line of sight (projected distance 1.2–1.3 arcsec, or $\simeq$ 10 kpc at the absorber redshift). We argue that, given the small probability of a chance alignment and the implied impact parameter at $z_{\rm abs}$, these two objects are promising candidates for the DLA absorption. Both would have luminosities close to L^*_K and their properties would be consistent with trends identified in metal line absorber galaxies found at lower redshifts.

2. The radial distribution of faint sources around the QSOs shows good agreement with that expected from published K-band number counts for projected distances $\gtrsim$ 7 arcsec. At $\theta \lesssim 7$ arcsec, radio quiet QSOs show no sign of excess in the number of objects, but the radio loud QSOs show an excess of 2.8 sources per line of sight significant at the 99.5% level.

3. Recognising that the statistical significance of the excess is not very high given the number of lines of sight sampled, the difference in behaviour detected for the radio quiet and radio loud QSOs is nonetheless suggestive. Since the DLA systems should not be affected by the radio properties of the QSOs ($z_{\rm abs} \ll z_{\rm em}$), we suggest the excess may be associated with the QSOs themselves. If that is the case, radio loud QSOs at $z \simeq 2.4$ could well reside in groups or clusters of galaxies much in the same way as closer counterparts, and we are just seeing the 2–3 brightest galaxies there.

4. The average luminosity of the excess galaxies, if placed at $z_{\rm em}$, is $\simeq 2L^*_K$, and the magnitude distribution reaches $\simeq 2$ mag brighter than L^*_K. If these galaxies are the high redshift counterparts of present day brightest cluster galaxies, it implies luminosity evolution in the K-band of ~ 1 mag from $z \simeq 2.4$ to the present, in the sense that high-z galaxies were brighter than today.

Imaging high redshift QSO sightlines is an efficient method to identify likely high-z galaxies for evolutionary studies. To the precision where evolutionary comparison with lower redshift galaxies are concerned, the small difference in look-back-time makes it immaterial whether the galaxies are at $z_{\rm abs}$ or at $z_{\rm em}$. A larger sample of radio loud and radio quiet QSOs, with and without DLA systems is needed in order to add weight to our statistical conclusions. Once the excess is firmly established, HST imaging would provide morphology and colours and be useful in searching for objects even closer to the QSO line of sight. Obtaining redshifts can resolve the ambiguities and this may be practical shortly via the use of near-infrared spectrographs offering OH-suppression where faint emission lines may be seen against the contrast of the strong infrared background .

ACKNOWLEDGEMENTS

We would like to thank UKIRT staff for their assistance in securing these observations, and Guinevere Kauffman, James Lowenthal and Simon White for very useful discussions. We are also grateful to Mark Dickinson, the referee of this paper, for his comments. AAS acknowledges generous financial support from the Royal Society.

REFERENCES

Aragón-Salamanca, A., Ellis, R.S., Schwartzenberg, J.-M. & Bergeron, J. 1994, ApJ, 421, 27.
Bahcall, J.N. & Peebles, P.J.E., 1969, ApJ, 156, L7.
Barger, A.J., Aragón-Salamanca, A., Ellis, R.S., Couch, W.J., Smail, I. & Sharples, R.M. 1995, MNRAS, in press.
Beers, T.C., Flynn, K, & Gebhard, K. 1990, AJ, 100, 32.
Bergeron, J. & Boissé, P. 1991, A&A, 243, 344.
Casali, M. & Hawarden, T. 1992, The UKIRT–JCMT Newsletter, 4, 33.
Cowie, L.L., Hu. E.M. & Songaila, A., 1995, Nature, 377, 603.
Ellingson, E., Yee, H.K.C. & Green, R.F. 1991, ApJ, 371, 36.
Ellis, R.S. 1995, in Unsolved Problems in Astrophysics, eds. J.P. Ostriker & J.N. Bahcall, (Princeton: Princeton University Press), in press.
Ellis, R. S., Colless, M., Broadhurst, T. J., Heyl, J. & Glazebrook, K. 1995, MNRAS, in press.
Elston, R., Bechtold, J., Lowenthal, J. & Rieke, M. 1991, ApJ, 373, L39.
Gardner, J.P., Cowie, L.L. & Wainscoat, R.J. 1993, ApJ, 415, L9.
Hewitt, A. & Burbidge, G. 1993, ApJS, 87, 451.
Irwin, M.J. 1985, MNRAS214, 575.
Junkkarinen, V., Hewitt, A. & Burbidge, G. 1991, ApJS, 77, 203.
Lilly, S.J. Tresse, L., Hammer, F., Crampton, D., Le Fevre, O., 1995, ApJ, in press.
Mobasher, B., Sharples, R.M. & Ellis, R.S. 1993, MNRAS, 263, 560.
Rao, S. & Briggs, F.H. 1993, ApJ, 419, 515.
Steidel, C., Dickinson, M. & Persson, S.E., 1994, ApJ, 437, L75.
Steidel, C., Pettini, M., Dickinson, M. & Persson, S.E. 1994, AJ, 108, 2046.
Steidel, C. & Dickinson, M., 1995, in Wide Field Spectroscopy and the Distant Universe, eds. S.J. Maddox & A. Aragón-Salamanca, (Singapore: World Scientific), 349.
Wolfe, A.M, Turnshek, D.A., Smith, H.E. & Cohen, R.D. 1986, ApJS, 61, 249.
Wolfe, A.M, Turnshek, D.A., Lanzetta, K.M. & Lu, L. 1993, ApJ, 404, 480.
Yanny, B. & York, D.G. 1992, ApJ, 391, 569.
Yee, H.K.C. & Green, R.F. 1987, ApJ, 319, 28.